Journal of The Electrochemical Society, **146** (8) 2780-2783 (1999)
S0013-4651(98)11-014-5 CCC: $7.00 © The Electrochemical Society, Inc.

Vanadium Oxide Nanotubes

A New Nanostructured Redox-Active Material for the Electrochemical Insertion of Lithium

Michael E. Spahr,[a,b,c] Petra Stoschitzki-Bitterli,[b] Reinhard Nesper,[b] Otto Haas,[a,*] and Petr Novák,[a,z]

[a]*Paul Scherrer Institute, Electrochemistry Section, CH-5232 Villigen PSI, Switzerland*
[b]*Swiss Federal Institute of Technology (ETH), Laboratory of Inorganic Chemistry, ETH-Zentrum, CH-8092 Zurich, Switzerland*

Vanadium oxide nanotubes were prepared in a modified sol-gel reaction of vanadium oxide triisopropoxide conducted in the presence of the structurally directing hexadecylamine and followed by hydrothermal treatment. The tubes consist of concentric shells of highly crystalline vanadium oxide separated by alternating organic amine layers. The template molecules were removed without structural breakdown of the nanotubes by a combined ion-exchange reaction and extraction process. The vanadium oxide nanotubes are redox-active and can electrochemically insert lithium reversibly. A specific charge up to 180 mAh g^{-1} (with respect to the oxide) was measured for Li^+ insertion into porous electrodes containing template-free nanotubes. The specific charge decreased during cycling, indicating a loss of electroactivity.

Manuscript submitted November 2, 1998; revised manuscript received March 23, 1999.

Materials with nanosized structures belong to a rapidly growing field of contemporary scientific interest. Nanostructured materials are understood to be intermediates between the classical molecular scale and microsized entities.[1,2] Chemical structures and systems within the size range from about 1 to 100 nm in one, two, or three dimensions are typical for such materials. They are attracting considerable attention, because they present new challenges for the chemist, they frequently exhibit novel properties, and some nanoscale systems offer interesting device applications as a consequence of their size, properties, and topology.

Micelle-based chemical synthesis is a known approach yielding nanoparticles with well-defined dimensions.[3] However, in most other cases well-defined nanoscaled structures are difficult to obtain, because neither physical tailoring techniques nor planned chemical syntheses go very far into this size domain. Nanoparticles are much more reactive than the corresponding macroscopic bulk material, and their physical properties become a sensible function of their size. The nanoscale dimensions imply a very high fraction of atoms residing at nanocrystalline grain boundaries. The high specific surface area of these materials has significant implications with respect to energy storage devices based on electrochemically active sites (batteries, supercapacitors) and energy conversion devices depending on catalytic sites or defect structure (fuel cells and thermoelectric devices).[4,5]

Discovered in 1991 by Iijima, carbon nanotubes are popular representatives of this group of materials.[6] Depending on the synthesis conditions in arc-discharge experiments between carbon electrodes, either single- or multiwalled tubes consisting of graphite-related sheets are formed.[6-9] Carbon nanotubes have diameters in the order of 10 to 30 nm. The tube diameter and the tube geometry determine whether the nanotubes behave electronically like a metal or a semiconductor. It is possible to insert lithium into carbon nanotubes either chemically or electrochemically, leading to lithiated carbon compounds with compositions of up to LiC_3.[10] This very high lithium content raises expectations for carbon nanotubes as a possible negative electrode material for lithium-ion batteries.

Our goal was to synthesize a material with a structure similar to carbon nanotubes, but with a much more positive redox potential, which could conceivably function as electroactive material for positive electrodes in secondary lithium batteries. Lithium-inserting oxides are normally used in such electrodes.[11] Recently, we reported the directed chemical synthesis of tubular-shaped vanadium oxide nanotubes using the templating effect of self-assembled surfactant molecules in a modified sol-gel process.[12,13] These vanadium oxide nanotubes consist of several concentric shells similar to the analogous but smaller multiwalled carbon tubes. The nanotube structure of the vanadium oxide could be preserved even after removing the template molecules.

The shapes of both template-containing and template-free nanotubes attract much scientific interest: a tube has a very advantageous shape offering three generally different contact regions, namely, the inner and outer wall surfaces as well as the tube ends. Especially for insertion processes, which are believed to be controlled by diffusion in the solid electroactive material, large inner and outer wall surfaces might be favorable because (*i*) the diffusion path in the solid is shorter and (*ii*) the heterogeneous kinetics are faster with higher surface-to-bulk ratios. Moreover, the tubes can provide electrolyte-filled channels for faster transport of the ions to the insertion sites. This paper is the first report on the electrochemical properties of an entirely new material with a unique nanostructured tubular morphology based on V_2O_5.

Experimental

The vanadium oxide nanotubes were prepared by stirring a solution of vanadium (V) oxide triisopropoxide and hexadecylamine in a molar ratio of 2:1 in ethanol under an inert gas for 1 h. Hydrolysis of the reaction mixture under vigorous stirring followed by aging of the hydrolysis product led to a yellow suspension of surfactant and a hydrolyzed vanadium oxide component. Heating the hydrolysis mixture under hydrothermal conditions at 180°C at a pressure of <10 bar for about 1 week gave vanadium oxide nanotubes. The nanotubes were the only product detected. After the hydrothermal treatment the color of the materials changed to black. The black material was filtered and then washed with water, ethanol, and diethyl ether. The vanadium oxide was refluxed in a saturated solution of NaCl in ethanol for 24 h in order to remove the hexadecylamine template. Then the material was filtered, washed thoroughly with ethanol, and dried under high vacuum at room temperature.

Chemical analysis was performed by C, H, and N microelement analyses and thermogravimetric analysis (Perkin Elmer TGA P 7). The metal contents were determined by induced coupled plasma atomic emission spectroscopy (ICPAES, Zeiss Plasmaquant 101). Transmission electron microscopic (TEM) and scanning electron microscopic (SEM) characterization of the samples was carried out on a Philips CM30. The Brunauer, Emmett, Teller (BET) specific surface area measurements were performed with a Micromeritics ASAP 2000 using nitrogen as adsorption gas. X-ray powder diffraction (XRD) was carried out with a STOE diffractometer using Cu $K\alpha_1$ radiation (λ = 1.54056 Å).

* Electrochemical Society Active Member.
[c] Present address: TIMCAL AG, CH-5643 Sins, Switzerland.
[z] E-mail: Petr.Novak@psi.ch

S0013-4651(98)11-014-5 CCC: $7.00 © The Electrochemical Society, Inc.

Magnetic susceptibility measurements were performed in a constant magnetic field of 1000 G using a SQUID magnetometer (Quantum Design MPM 5S) as described in Ref. 14. A correction was introduced for the contribution of the quartz sample holder to the total magnetic susceptibility.

Electrochemical experiments were carried out with porous working electrodes mounted in hermetically sealed laboratory cells with a three-electrode arrangement, as described in detail elsewhere.[15,16] The vanadium oxide nanotubes were mixed with an equal weight of Teflonized carbon black (25 wt % polytetrafluoroethylene and 75 wt % acetylene black), and the mixture was pressed on a titanium current collector. The working electrode had a geometric surface area of 1.3 cm^2 and contained approximately 10 mg of the vanadium oxide material. Both the specific current and the specific charge are given with respect to the weight of the oxide in the porous electrode. The working and counter electrode were slightly mechanically pressed together against a glass fiber separator soaked with the electrolyte, 1 M $LiClO_4$ in propylene carbonate (PC). Metallic lithium served as counter and reference electrode. The cycling was performed with standard electrochemical instrumentation.

Results and Discussion

Characterization of the nanotube material.—According to chemical analysis, the black, needle-like vanadium oxide which was isolated from the hydrothermal reaction has the nominal composition of $VO_{2.45}(TEMP)_{0.34}$ (TEMP = $C_{16}H_{33}NH_2$), indicating that a relatively large amount of organic template was built into the oxide structure during synthesis. The black material was paramagnetic and showed a semimetallic conductivity, presumably due to mixed-valence vanadium centers. Magnetic susceptibility measurements revealed a fraction of about 5% vanadium(IV) besides vanadium(V) in the material, indicating a slight reduction of vanadium(V) during the hydrothermal reaction. This explains the color change from orange (V_2O_5) to black ($V_y^{4+}V^{5+}O_x$) because mixed-valent V(IV,V) oxides are generally black (*e.g.*, V_6O_{13}).

For the template-containing material, electron microscopy showed nanotubes with lengths of up to a few micrometers, both isolated and grown together. As can be seen from the TEM images in Fig. 1 and 2, the tubes consisted of several concentric shells, each about 2.8 to 3 nm in thickness. The same shell thickness of about 3 nm was evaluated from the most pronounced intensity maximum found in the very broad X-ray patterns (Fig. 3). The external tube diameters fell between 15 and 100 nm and the internal diameters were between 5 and 50 nm, whereas the tube wall thicknesses were typically between 5 and 25 nm. The SEM image in Fig. 4 illustrates the open-ended cylindrical shape of the tubes. The BET specific surface area was about 80 $m^2\ g^{-1}$, which seems to be fairly low, however, there is evidence for residual solvent molecules covering parts of the surface area. From both the TEM images and stoichiometry of the material we conclude that the tubes consist of concentric shells of highly crystalline vanadium oxide separated by alternating organic amine layers.

The template-free nanotubes exhibit a reduced shell thickness of about 0.86 nm, as shown in the high-resolution TEM image in Fig. 5. Surface contrasts with a periodicity of about 0.65 nm are observed within the individual shells, indicating an ordered structure of the

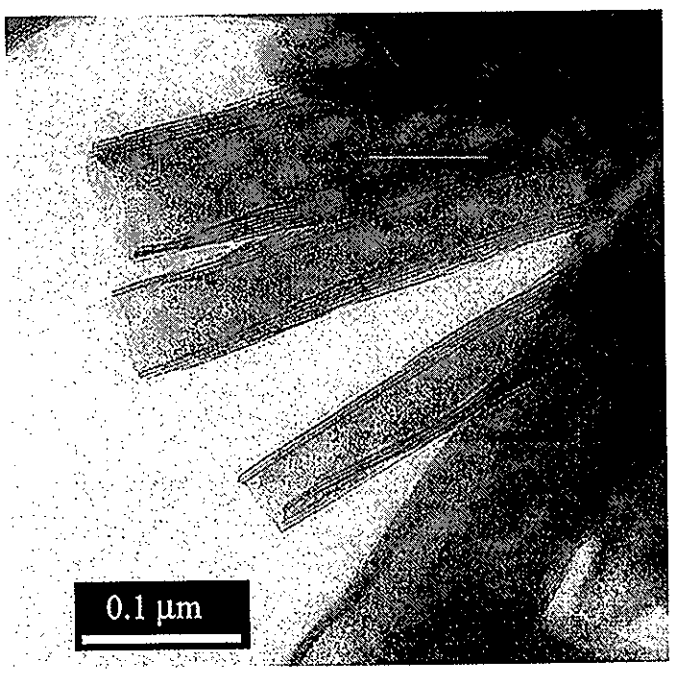

Figure 1. TEM image of vanadium oxide nanotubes with the composition $VO_{2.45}(TEMP)_{0.34}$ (TEMP = $C_{16}H_{33}NH_2$), synthesized by a directed process via a modified sol-gel reaction.

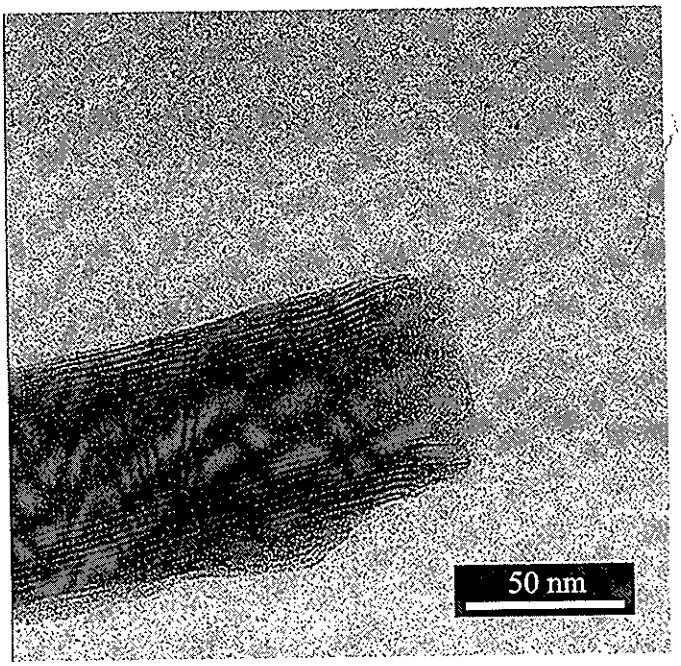

Figure 2. TEM image of a template-containing vanadium oxide nanotube showing the typical open end.

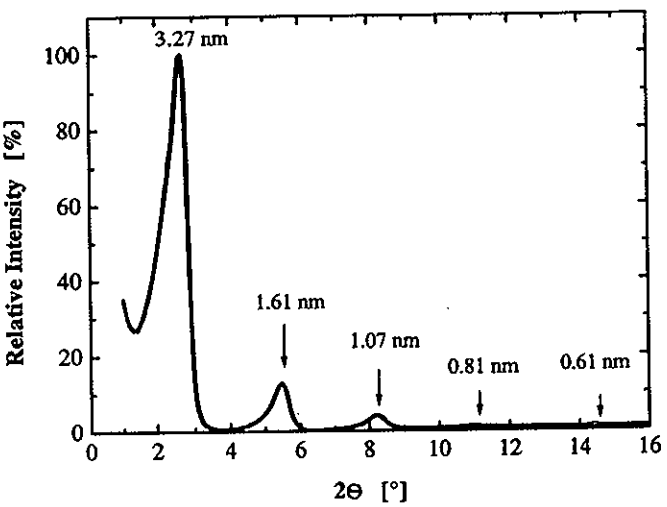

Figure 3. Powder XRD pattern of the vanadium oxide nanotubes containing the hexadecylamine as template.

Journal of The Electrochemical Society, **146** (8) 2780-2783 (1999)
S0013-4651(98)11-014-5 CCC: $7.00

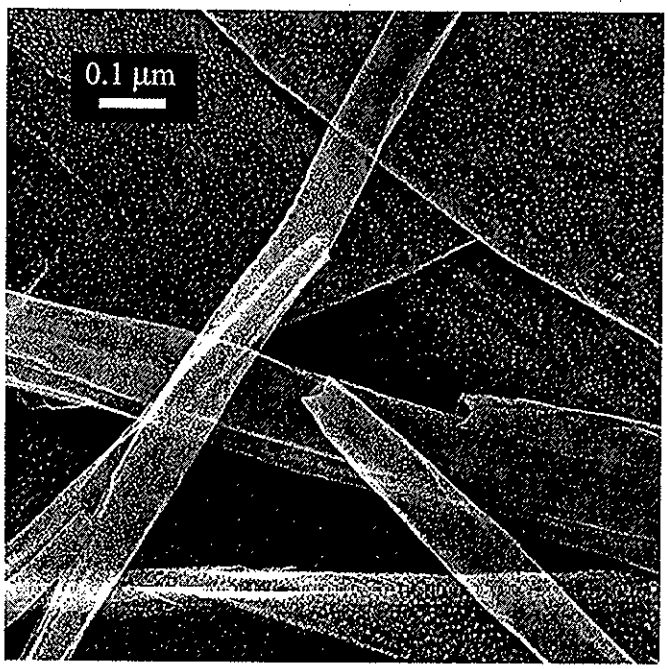

Figure 4. SEM image of the template-containing vanadium oxide illustrating its nanotubular morphology with open ends.

vanadium oxide. A BET specific surface area of about 35 $m^2\ g^{-1}$ was measured for the template-free material, which is a significantly lower value than that found for the template-containing material.

Electrochemical measurements.—To ensure each oxide particle a good contact and at the same time a sufficient electrode porosity, the electrochemical characterization of the vanadium oxide nanotubes was performed with electrodes consisting of a mixture of the oxide with 50% Teflonized carbon black, as recommended in Ref. 16. Cyclic voltammograms of $VO_{2.45}(TEMP)_{0.34}$ and of the template-free vanadium oxide nanotubes in the potential range between 1.2 and 4.0 V *vs.* Li/Li^+ are shown in Fig. 6. The cathodic current observed for $VO_{2.45}(TEMP)_{0.34}$ at potentials more negative than 2 V vs. Li/Li^+ corresponds to the electrochemical insertion of lithium into the nanostructured material

$$x\mathrm{Li}^+ + x\mathrm{e}^- + \mathrm{VO}_{2.45}(\mathrm{TEMP})_{0.34} \rightleftarrows \mathrm{Li}_x\mathrm{VO}_{2.45}(\mathrm{TEMP})_{0.34}$$

The corresponding oxidation process begins at about 3 V *vs.* Li/Li^+, indicating a kinetically hindered reoxidation of the material. A rather stable specific charge of about 120 mAh g^{-1} was obtained for the Li^+ insertion during the first five cycles of voltammetric measurements at 50 μV s^{-1}. Thereafter, the specific charge gradually decreased with increasing cycle number to less than 100 mAh g^{-1} after ten cycles.

The shape of the cyclic voltammogram changed drastically when the template was removed from the nanotubes. The electrochemical lithium insertion proceeded at potentials more negative than 3 V *vs.* Li/Li^+ in two additional reduction processes (Fig. 6). A specific charge of about 180 mAh g^{-1} was obtained for Li^+ insertion during the first potentiodynamic reduction half-cycle. The Li^+ insertion was fairly reversible, as can be seen from the corresponding broad oxidation peak with a maximum at about 2.7 V *vs.* Li/Li^+. The significant difference in specific charge as well as in the shape of the voltammogram between the template-containing and template-free materials indicates that the organic amine molecules are involved in the electrochemical cycling of the former, or at least contribute to a partial passivation of the nanotubes.

The first three voltammetric cycles of the template-free vanadium oxide nanotubes are shown in Fig. 7. The change in shape of the voltammogram with cycle number indicates a change of the material

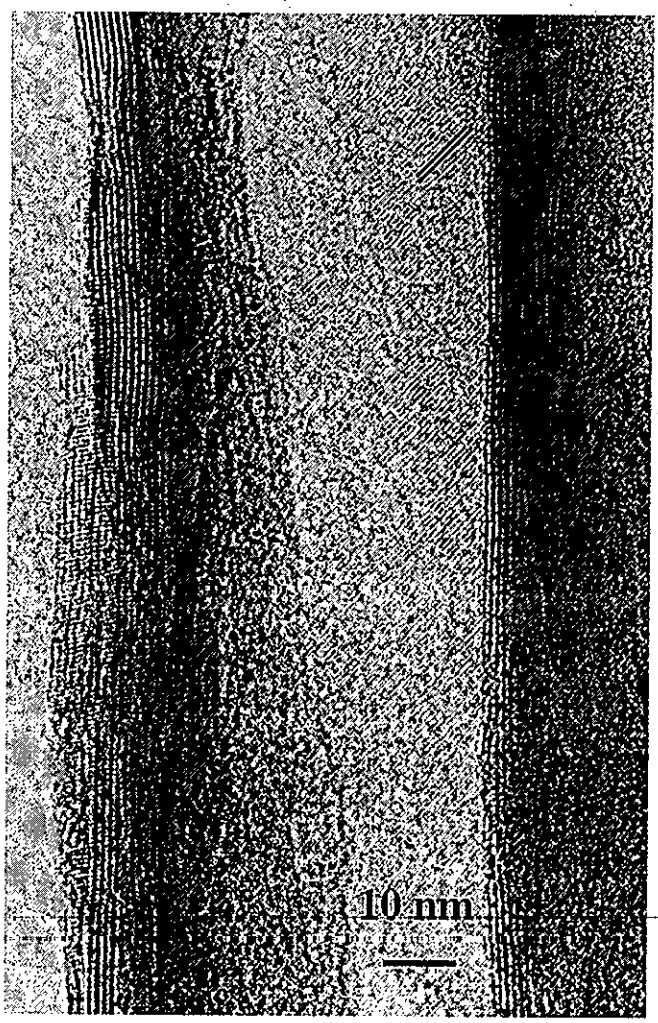

Figure 5. High-resolution TEM image of a template-free nanotube consisting of concentric shells of crystalline vanadium oxide. The contrasts along the walls exhibit a distance of about 0.86 nm. Several regions show a fine structure with contrast distances of about 0.65 nm (see the // mark in the image), which are indicative of an ordered structure between the individual shells of the tube wall.

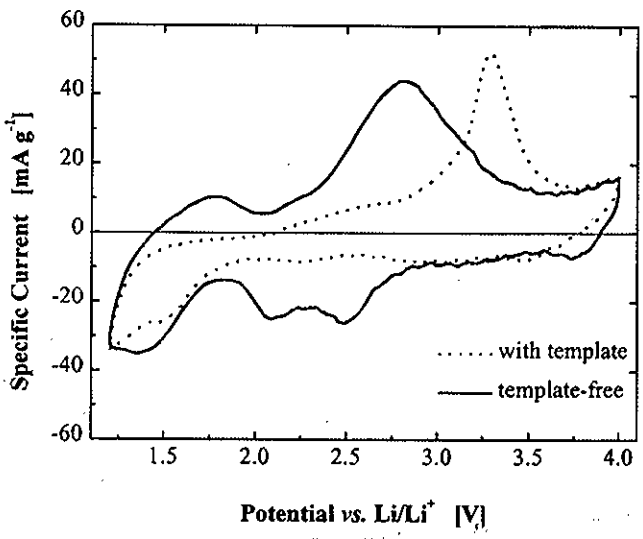

Figure 6. Cyclic voltammograms of the template-containing and template-free vanadium oxide nanotubes recorded at 50 μV s^{-1} in 1 M $LiClO_4$/PC. The electrodes contained 50 wt % Teflonized carbon black.

S0013-4651(98)11-014-5 CCC: $7.00 © The Electrochemical Society, Inc.

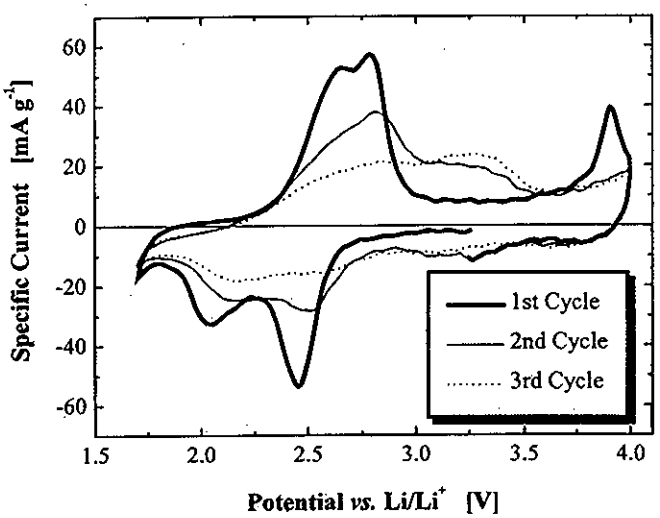

Figure 7. 1st, 2nd, and 3rd voltammetric cycle at 50 μV s^{-1} of the template-free vanadium oxide nanotubes.

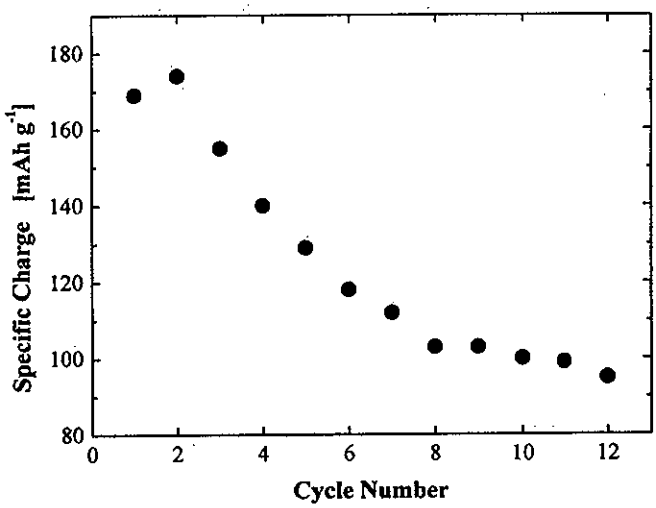

Figure 8. Dependence of the specific charge on the cycle number obtained from potentiodynamic measurements at 50 μV s^{-1} in the potential window from 1.5 to 4.0 V *vs.* Li/Li$^+$.

during cycling, the material has lost electroactivity to some extent. The most likely reason is the amorphization and/or other structural changes of the material upon cycling. Further evidence for an irreversible change occurring with the nanotubes is the irreversible oxidation peak appearing in the first voltammetric cycle at a potential of about 3.8 *vs.* Li/Li$^+$. The specific charge of nearly 180 mAh g^{-1} obtained for Li$^+$ insertion decreases with increasing cycle number, as illustrated in Fig. 8.

Conclusions

We demonstrated that it is possible to synthesize template-free, redox-active vanadium oxide nanotubes. This entirely new material with a unique nanostructured morphology can electrochemically insert/deinsert lithium ions. However, the material changes during cycling. Thus, further investigations are needed before the properties of this new material will be fully understood and practical applications realized.

Acknowledgments

The partial financial support by the Swiss Federal Office of Energy, Bern, is gratefully acknowledged. Dr. M. Müller and Dr. F. Krumeich, both of the Swiss Federal Institute of Technology (ETH Zurich) are thanked for the electron microscopy images. Thanks are also due to K. Hametner of the ETH Zurich and F. Geiger of the Paul Scherrer Institute for materials analysis and for BET measurements, respectively.

Paul Scherrer Institute assisted in meeting the publication costs of this article.

References

1. Leading reviews: (a) G. M. Whitesides, J. P. Mathias, and C. T. Seto, *Science*, **254**, 1312 (1991); (b) G. A. Ozin, *Adv. Mater.*, **4**, 612 (1992); (c) D. Philp and J. F. Stoddart, *Angew. Chem., Int. Ed. Engl.*, **35**, 1155 (1996).
2. *Chem. Mater.*, Special Issue on Nanostructured Materials, **8**, 1569 (1996).
3. J. Y. Ying, C. P. Mehnert, and M. S. Wong, *Angew. Chem., Int. Ed. Engl.*, **38**, 56 (1999).
4. M. Nishizawa, K. Mukai, S. Kuwabata, C. R. Martin, and H. Yoneyama, *J. Electrochem. Soc.*, **144**, 1923 (1997).
5. G. Che, K. B. Jirage, E. R. Fisher, C. R. Martin, and H. Yoneyama, *J. Electrochem. Soc.*, **144**, 4296 (1997).
6. S. Iijima, *Nature*, **354**, 56 (1991).
7. S. Iijima and T. Ichihashi, *Nature*, **363**, 603 (1993).
8. T. W. Ebbesen and P. M. Ajayan, *Nature*, **358**, 220 (1992).
9. D. S. Bethune, C. H. Kiang, M. S. de Vries, G. Gorman, R. Savoy, J. Vasquez, and R. Beyers, *Nature*, **363**, 605 (1993).
10. G. Che, B. B. Lakshmi, E. R. Fisher, and C. R. Martin, *Nature*, **393**, 346 (1998).
11. M. Winter, J. O. Besenhard, M. E. Spahr, and P. Novák, *Adv. Mater.*, **10**, 725 (1998).
12. M. E. Spahr, P. Stoschitzki-Bitterli, R. Nesper, M. Müller, F. Krumeich, and H. U. Nissen, *Angew. Chem., Int. Ed. Engl.*, **37**, 1263 (1998).
13. R. Nesper, M. E. Spahr, M. Niederberger, and P. Stoschitzki-Bitterli, Pat. No. PCT/CH97/00470, WO 98/26871, Swiss Federal Institute of Intellectual Property, Bern, Switzerland (1998).
14. M. E. Spahr, P. Novák, B. Schnyder, O. Haas, and R. Nesper, *J. Electrochem. Soc.*, **145**, 1113 (1998).
15. P. Novák, W. Scheifele, F. Joho, and O. Haas, *J. Electrochem. Soc.*, **142**, 2545 (1995).
16. M. E. Spahr, P. Novák, O. Haas, and R. Nesper, *J. Power Sources*, **68**, 629 (1997).